

1 **Dielectrophoretic Detection of Electrical Property Changes**
2 **of Stored Human Red Blood Cells**

3 Edwin D. Lavi¹, Francesca Crivellari and Zachary Gagnon²

4
5 ¹ Department of Chemical Engineering, Texas A&M University, 3122 TAMU, College
6 Station TX, 77843.

7 ² Department of Chemical Engineering, Texas A&M University, 3122 TAMU, College
8 Station TX, 77843.

9
10 *Correspondence should be addressed to the following author:

11 Zachary Gagnon, Associate Professor

12 Department of Chemical Engineering

13 Texas A&M University

14 203 Jack E. Brown Engineering Building, College Station TX, 77843

15 zgagnon@tamu.edu

16
17 **Keywords:** dielectrophoresis, crossover frequency, electrophysiology, human red
18 blood cells, glutaraldehyde

19 **Abbreviations:** crossover frequency (COF), glutaraldehyde (glt)

20

21 **Abstract**

22 The ability to transport and store a large human blood inventory for transfusions is an
23 essential requirement for medical institutions. Thus, there is an important need for
24 rapid and low-cost characterization tools for analyzing the properties of human red
25 blood cells (RBCs) while in storage. In this study, we investigate the ability to use
26 dielectrophoresis (DEP) for measuring the storage-induced changes in RBC electrical
27 properties. Fresh human blood was collected, suspended in K2-EDTA anticoagulant
28 and stored in a blood bank refrigerator for a period of 20 days. Cells were removed
29 from storage at 5-day intervals and subjected to a glutaraldehyde crosslinking reaction
30 to “freeze” cells at their ionic equilibrium at that point in time and prevent ion leakage
31 during DEP analysis. The DEP behavior of RBCs was analyzed in a high permittivity
32 DEP buffer using a three-dimensional DEP chip (3DEP) and also compared to
33 measurements taken with a 2D quadrupole electrode array. The DEP analysis
34 confirms that RBC electrical property changes occur during storage and are only
35 discernable with the use of the cell crosslinking reaction above a glutaraldehyde
36 fixation concentration of 1.0 w/v%. In particular, cytoplasm conductivity was observed
37 to decrease by more than 75% while the RBC membrane conductance was observed
38 to increase by more than 1000% over a period of 20 days. These results show that
39 the presented combination of chemical crosslinking and DEP can be used as rapid
40 characterization tool for monitoring electrical properties changes of human red blood
41 cells while subjected to refrigeration in blood bank storage.

42

43

44 **1 Introduction**

45 Subcellular components such as the lipid bilayer membrane, cytoskeleton, and
46 cytoplasm play essential roles in maintaining cellular function and cell health.
47 Environmental influences such as disease, exposure to pathogens, and
48 pharmacological interventions can impact the physiological characteristics and
49 structural organization of these subcomponents, which can influence their
50 biomechanical and bioelectrical properties. Electrical property changes have been
51 correlated with many physiological processes, including the differentiation state of
52 neural and embryonic stem cells [1,2]. During cell invasion and development, the
53 malaria inducing parasite, Plasmodium falciparum induces electrical changes in
54 human red blood cell (RBC) cytoplasm and membrane conductance [3].
55 Pharmacological interventions, such as cell exposure to ion channel blockers and anti-
56 cancer treatments have been shown to induce changes in cancer cell electrical
57 properties. Membrane potential has also shown to be an important indicator in
58 biological function, including during the progression of cancer [4]. Similarly, recent
59 studies demonstrate the significance of membrane conductance and cytoplasmic
60 conductivity in contributing to the regulation of the circadian rhythm in human red blood
61 cells [5] and in HL-60 cells undergoing apoptosis [6,7]. A significant and continuing
62 growing body of work therefore demonstrates that cellular electrical properties have
63 the potential to serve as label-free diagnostic markers in cell identification, disease
64 detection, cell separation and for health monitoring [1,8,9].

65 One important diagnostic marker is the quality of stored human blood for
66 transfusion [10]. Modern blood storage systems enable the donation and transfusion
67 of blood to be dynamically separated in time and space. Large medical centers can
68 use hundreds of units of RBCs a day, and the ability to transport and build large blood

69 storage inventory is an important requirement for medical institutions. However, such
70 readily available blood storage often raises the question: how long can blood be stored
71 before it is no longer safe and effective for blood transfusions?

72 RBCs show clear signs of degradation during storage, and there are many
73 known physiological changes associated with RBC storage, including changes in cell
74 morphology and loss of metabolism [11]. A number of RBC quality measures exist,
75 including measuring hemoglobin concentration in RBC storage and measuring the
76 potassium ion concentration in suspension solution, however, no such methods
77 quantify the electrical properties of the RBCs themselves. One metric related to cell
78 electrical properties is the diffusive loss of cytoplasmic cations, such as K^+ , Na^+ and
79 Ca^{2+} via the cell membrane while the blood is stored under refrigeration in a blood
80 bank. In particular, the activity of the sodium-potassium ion pump is highly sensitive to
81 temperature, and refrigerated RBCs have been shown to leak potassium into their
82 suspending buffer during storage [12]. When reinfused, cells have the potential to
83 reabsorb potassium which can alter the local extracellular potassium concentration. In
84 cases with an infant or when a large volume of blood relative to the patient's circulating
85 volume is required, such ion reabsorption can lead to death [12]. Development of low-
86 cost and rapid methods to dynamically track the electrical properties of human red
87 blood cells in storage could therefore play an important role in dynamically monitoring
88 the health of stored blood.

89 One method to measure cell electrical properties is to use the electrokinetic
90 technique, dielectrophoresis (DEP) [13]. Conventionally, DEP is performed using two-
91 dimensional (2D) thin-film electrode arrays with quadrupole, interdigitated, comb-tooth
92 or castellated structures that are typically fabricated atop a glass substrate and
93 observed under an optical microscope. Cells suspended in a buffer of known electrical

94 conductivity and permittivity are deposited on the electrode array and subjected to a
95 sweeping electric-field frequency. The electric field from the electrodes polarizes the
96 cells and dielectrophoretically drives them to spatially assemble within the confines of
97 the electrode array. The specific geometric location of the DEP cell assembly is based
98 on cell and buffer electrical properties and the AC field frequency; cells will experience
99 a different DEP force - both in direction and magnitude - depending on the frequency
100 applied. The resulting frequency dependent DEP force curve, or DEP spectrum, will
101 consist of finite field frequency ranges where cells are either attracted towards
102 (positive DEP) or repelled away from (negative DEP) the high electric field regions as
103 defined by the array's electrodes. The frequency in which this attraction/repulsion
104 reverses and cell DEP motion ceases is defined as the DEP crossover frequency
105 (COF). The frequency dependent DEP behavior can be measured optically and
106 combined with an appropriate Maxwell-Wagner cell polarization model to empirically
107 deduce cell electrical properties. In this manner, the entire cell suspension is utilized
108 to measure the COF and therefore the resulting DEP method yields electrical
109 properties reflective to the mean value of the entire cell suspension under observation.

110 While the 2D electrode array method is effective and responsible for many
111 impactful contributions within the DEP community, it does suffer from several
112 limitations. First, this method typically requires one to manually observe DEP-induced
113 cell trajectories. This process requires a highly trained operator and can be tedious for
114 large numbers of samples. Further this manual method is vulnerable to human error
115 and bias. Second, very often this method is only useful in measuring cell COFs which
116 represents single data points within the entire DEP spectrum. Therefore, significant
117 experimental data and DEP behavior in the positive and negative DEP frequency
118 ranges of the spectrum are often not taken into consideration. Such a constraint places

119 a limit on the ability to accurately correlate DEP behavior to DEP polarization theory
120 and determine the cell electrical properties. In an effort to overcome the drawbacks of
121 conventional 2D experiments and to realize DEP as a more formal analytical tool,
122 Hughes et al. developed the 3DEP dielectrophoretic cytometer [14]. The 3DEP is
123 capable of measuring a more complete DEP force spectrum and empirically calculate
124 the cell suspension electrical properties.

125 In this work, we demonstrate the use of DEP to quantify the storage-induced
126 electrical property changes of human RBCs subjected to blood-bank refrigeration. In
127 order to minimize ion leakage across the RBC membrane during DEP measurements,
128 we utilize a glutaraldehyde crosslinking reaction prior to cell washing and suspension
129 in a low conductivity-high permittivity zwitterion DEP buffer [15–17]. The
130 glutaraldehyde crosslinks aminated protein groups and serves to inhibit ion loss
131 through the membrane, while the zwitterion buffer reduces the second high frequency
132 DEP COF to within the operating range of most standard function generators. We
133 analyzed the influence of varying concentrations of glutaraldehyde on the DEP
134 behavior of human RBCs over a period of 20 days and used the 3DEP to calculate the
135 cell electrical properties. We also analyzed and compared the DEP spectrum obtained
136 by the 3DEP with that of a 2D quadrupole electrode array in order to ensure these two
137 methods do indeed provide comparable experimental COFs. Results suggest that the
138 3DEP method is capable of discerning storage-induced electrical property changes of
139 human RBCs. With further development, we believe this glutaraldehyde-3DEP
140 approach can potentially offer a rapid low-cost method for electrically quantifying the
141 status of blood stored for transfusions and for detecting autologous blood transfusions
142 in doping/cheating endurance athletes.

143 2 Theory

144 2.1 DEP-Shell Model

145 We utilize DEP to investigate the dynamic changes of RBC electrical properties
146 when subjected to storage at 4 °C in a blood bank refrigerator over a period of 20 days.
147 The DEP force and polarization equation can be derived for a homogeneous
148 axisymmetric spherical particle and then modified for a RBC. The DEP force on a
149 spherical particle suspended in an electrolyte media is given as [18,19]:

$$150 \vec{F}_{\text{DEP}} = 2\pi\epsilon_o\epsilon_m r^3 \text{Re}[K(\omega)] \nabla \vec{E}^2, \quad (1)$$

151 where ϵ_o , ϵ_m , r and $\nabla \vec{E}^2$, is the permittivity of free space, dielectric constant of the
152 media, the radius of the particle and the gradient of the electric field squared, and $\text{Re}[\cdot]$
153] represents the real part of a complex variable. $K(\omega)$ is the Clausius-Mossotti factor
154 (CMF),

$$155 K(\omega) = \left[\frac{\epsilon_p^* - \epsilon_m^*}{\epsilon_p^* + 2\epsilon_m^*} \right]. \quad (2)$$

156 Physically, Eq. (2) describes the frequency dependent particle dipole moment, and is
157 based on a complex permittivity of both the particle, ϵ_p^* and media, ϵ_m^* . This factor
158 describes the frequency dependent polarization, and ultimately the direction a particle
159 will move in a field gradient under DEP. The DEP COF, for example occurs at a
160 frequency such that $\text{Re}[K(\omega)] = 0$, while the particle exhibits positive DEP (pDEP) and
161 negative DEP (nDEP) when $\text{Re}[K(\omega)] > 0$ and $\text{Re}[K(\omega)] < 0$, respectively.

162 Electrically, each domain – the particle and surrounding electrolyte - is modelled
163 as a leaky dielectric which behaves as an equivalent resistor and capacitor in series.
164 For a harmonic AC field with an angular frequency, ω this circuit exhibits a complex
165 permittivity, ϵ^* as

$$166 \epsilon^* = \epsilon - i \frac{\sigma}{\omega}, \quad (3)$$

167 which has a real part composed of the permittivity, ε and an imaginary part ($i^2 = -1$)
 168 that is a function of the angular field frequency, ω , and the electrical conductivity, σ .

169 Here, we consider the DEP force acting on a dilute suspension of human RBCs.
 170 The DEP particle force equation must be modified to account for the outer RBC
 171 membrane and inner cytoplasmic domain. Based on previous DEP work, we assume
 172 each individual human RBC is modelled as sphere of cytoplasm with an interior radius,
 173 r_1 surrounded by a shell of cell membrane with an outer radius, r_2 as determined by
 174 the cell membrane thickness. The polarization characteristics of both domains are
 175 captured with an effective complex permittivity term, ε_{eff}^* and can be shown to be
 176 [18,19]:

$$177 \quad \varepsilon_{eff}^* = \varepsilon_{mem}^* \frac{\left(\frac{r_2}{r_1}\right)^3 + 2\left(\frac{\varepsilon_{cyto}^* - \varepsilon_{mem}^*}{\varepsilon_{cyto}^* + 2\varepsilon_{mem}^*}\right)}{\left(\frac{r_2}{r_1}\right)^3 - \frac{\varepsilon_{cyto}^* - \varepsilon_{mem}^*}{\varepsilon_{cyto}^* + 2\varepsilon_{mem}^*}}, \quad (4)$$

178 where ε_{eff}^* replaces ε_p^* equation (Eq. 2). This effective term is a function of the electrical
 179 properties of both cell domains with a complex permittivity of the cytoplasm, ε_{cyto}^* and
 180 the cell membrane, ε_{mem}^* .

181 It is worth briefly justifying our assumption to use a spherical polarization model
 182 as an approximation for capturing the DEP behavior of an inherently non-spherical
 183 biconcave shaped human RBC. An alternative single-shelled DEP model utilizes an
 184 oblate spheroid to capture the RBC disc shaped geometry. In some instances, this
 185 oblate model is necessary to properly fit DEP polarization data, as was shown
 186 previously using bovine RBCs [21]. Using the opensource DEP spectrum software,
 187 myDEP [20] one can show that a single-shelled spherical DEP model for this study
 188 largely captures the DEP spectrum – including both low and high COFs – produced
 189 from an oblate spheroidal polarization model to within ~90% accuracy. It should be

190 noted that the 3DEP commercial instrument software is not yet capable of performing
191 regression analysis and data fitting with a non-spherical model. Therefore, while it is
192 the only existing option within the instrument, it is still important to validate the use of
193 a spherical assumption for any given cell system. Based on our DEP spectra
194 comparisons, we believe a spherical assumption is a valid DEP approximation for
195 human RBCs (experimentally measured mean radius, $r_2 = 4.2 \mu\text{m} \pm 0.4$; membrane
196 thickness = 7 nm) for our DEP experimental system.

197 **3 Materials and methods**

198 We now describe the fabrication and operation of the 2D and 3DEP devices, the high
199 permittivity zwitterion DEP buffer and the RBC glutaraldehyde chemical crosslinking
200 workflow.

201 **3.1 Dielectrophoresis Devices**

202 DEP experiments were performed using two different experimental methods.
203 First, a more complete DEP spectrum (up to a field frequency of 45 MHz) was
204 determined using the commercial 3DEP instrument (DEPtech, Heathfield, UK).
205 Second, a 2D quadrupole electrode array was used to measure the cellular DEP COF
206 and subsequently compared to that of the 3DEP spectrum.

207 **3.2 3DEP Analysis**

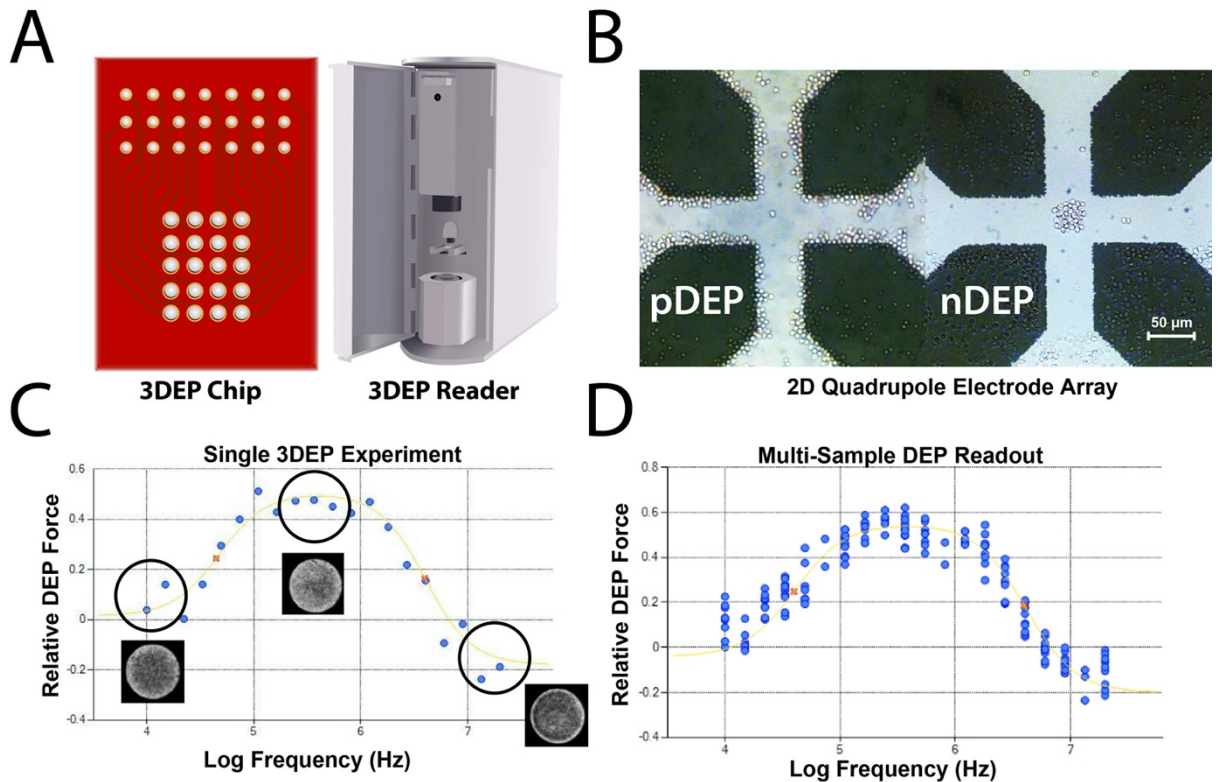
208 A detailed analysis of the operating theory and data analysis for the 3DEP has
209 been described elsewhere [14]. The 3DEP system consists of a printed circuit board
210 (PCB) chip which is inserted into a reader (Fig. 1A). The reader contains twenty
211 independent DDS-signal generators each capable of delivering a $20 V_{pp}$ waveform
212 source at frequencies up to 45 MHz. Each PCB 3DEP chip contains 20 small pinhole
213 wells capable of initiating DEP. The chip is illuminated using a collimated light source

214 and monitored using an integrated CMOS camera. When an electric field is applied to
215 each well, the resulting DEP force drives cell motion towards the well edges by pDEP,
216 or into the well center by nDEP depending on the frequency applied. The resulting
217 light intensity of each well is then used to compute a DEP force spectrum dataset (Fig.
218 1C). This process is repeated multiple times to increase the number of spectrum data
219 points and improve experimental accuracy (Fig. 1D). The 3DEP makes it possible to
220 measure the CMF of cells by monitoring the evolution of optical intensity passing
221 through each chip well. Each resulting 3DEP spectrum is a relative DEP force
222 spectrum and relates the CMF to the light intensity measured in each well through a
223 mathematical factor that remains unchanged during the course of the DEP experiment
224 [14]. The resulting spectrum is then not the complete DEP force, but instead is a
225 relative DEP force, or CMF, which can be used to deduce RBC electrical properties
226 by fitting these relative force spectra to the polarization model defined previously in
227 Eqns. 2 – 4.

228 **3.3 The Quadrupole Electrode Array**

229 2D quadrupole electrodes were fabricated using vapor deposition and wet
230 chemical etching techniques atop of thin glass coverslips (#1, 50 x 30 mm Fisher
231 Scientific). Each slide was coated with 20 nm of chromium and 30 nm of gold using
232 electron beam evaporation and subsequently patterned using a positive photoresist
233 (Shipley 1318). The exposed metal was then etched using gold and chromium
234 chemical etchant (Transene Company, Inc) to create a quadrupolar electrode array
235 geometry with four individual pointed electrodes, each with a separation lengthscale
236 of 50 μm and electrically accessible by a rectangular pad (Fig. 1B). A 20 V_{pp} voltage
237 over a varying frequency range was then applied to every other electrode using a
238 function generator (Rigol DG1022Z) while the other two non-active electrodes were

239 grounded. The voltage generated a well-defined high field region in the vicinity of the
240 electrode edges and a low field region in the center of the array. The DEP COF was
241 measured manually under brightfield microscopy by determining the field frequency in
242 which cell assembly transitioned from pDEP to that of nDEP (Fig. 1B).



243

244 **Figure 1. Dielectrophoresis Devices and Spectrum Analysis.** (A) 3DEP chip and
245 reader for measuring RBC DEP spectrum. (B) 2D quadrupolar array for DEP COF
246 measurements. RBCs collect at the electrode edges by pDEP or in the center by
247 nDEP depending on the AC frequency applied. (C) Relative DEP force spectrum
248 from a single experiment is fit to a single-shell spherical model. The circled
249 minima and maximum regions correspond to the DEP cell distributions within
250 the pictured 3DEP pinholes. (D) Multiple 3DEP sample repeats (N = 7)
251 superimposed and fit to the polarization model using regression analysis (R =
252 **0.9487**).

253

254

255 **3.4 Overview of Buffer and RBC Electrokinetic Optimization**

256 In this section we describe the preparation of our DEP buffer and the chemical
257 treatment of human RBCs for DEP analysis. Our overall strategy is to minimize as
258 much as feasible cytoplasmic leakage and interaction of a RBC interior with that

259 associated with resuspension in a high permittivity-low conductivity DEP buffer
260 immediately prior to DEP analysis. Therefore, in order to effectively capture the
261 storage related electrical property changes occurring in the RBCs we devised a
262 chemical crosslinking scheme to diffusively “seal” the interior cell cytoplasmic ionic
263 distribution during analysis in DEP buffer to more accurately elucidate RBC electrical
264 property changes that occurred while in refrigerated storage. Our previous work has
265 demonstrated that chemical crosslinking by the fixation agent, glutaraldehyde is an
266 effective approach to prevent cell leakage when cells are resuspended from
267 physiological buffer into a low conductivity DEP buffer [15,21]. Without a crosslinking
268 protocol, previous DEP studies with bovine RBCs showed that any storage induced
269 electrical changes were not resolvable by DEP [15,21]. After glutaraldehyde treatment
270 at the appropriate concentration, the chemically crosslinked cells are capable of
271 handling DEP analysis in low conductive DEP buffers without cytoplasmic leakage or
272 hemolysis. Therefore in this work, human RBCs were first treated with varying
273 concentrations of glutaraldehyde in order to chemically crosslink the aminated proteins
274 of the RBC and to determine the most effective concentration in which this effect is
275 observed with human blood. While we could attempt to instead use an osmotically
276 balanced DEP buffer as demonstrated in other DEP studies with human blood [5],
277 previous work with storage related DEP analysis has shown that it is important to
278 minimize the degree to which cells are capable of being osmotically influenced by a
279 change in buffer composition. Mass transport across the membrane during DEP
280 analysis has been shown to reduce DEP resolution and lead to dynamically changing
281 DEP behavior. Therefore, in this work we utilize chemical crosslinking to maximize
282 DEP resolution for detecting age related electrical changes in human RBCs.

283 In addition to chemically treating the RBCs, we also optimize our DEP buffer
284 with a polarizable zwitterionic salt in order to increase the buffer permittivity. In doing
285 so, the upper high frequency portion of the DEP spectrum associated with the second
286 DEP COF is shifted into a lower frequency space and within the full working range of
287 the 3DEP instrument. As such, a DEP spectrum which would normally require a > 60
288 MHz bandwidth to fully observe only requires an upper frequency of ~ 20 MHz. The
289 following sections below describe the chemical cell crosslinking and DEP buffer
290 preparation protocols.

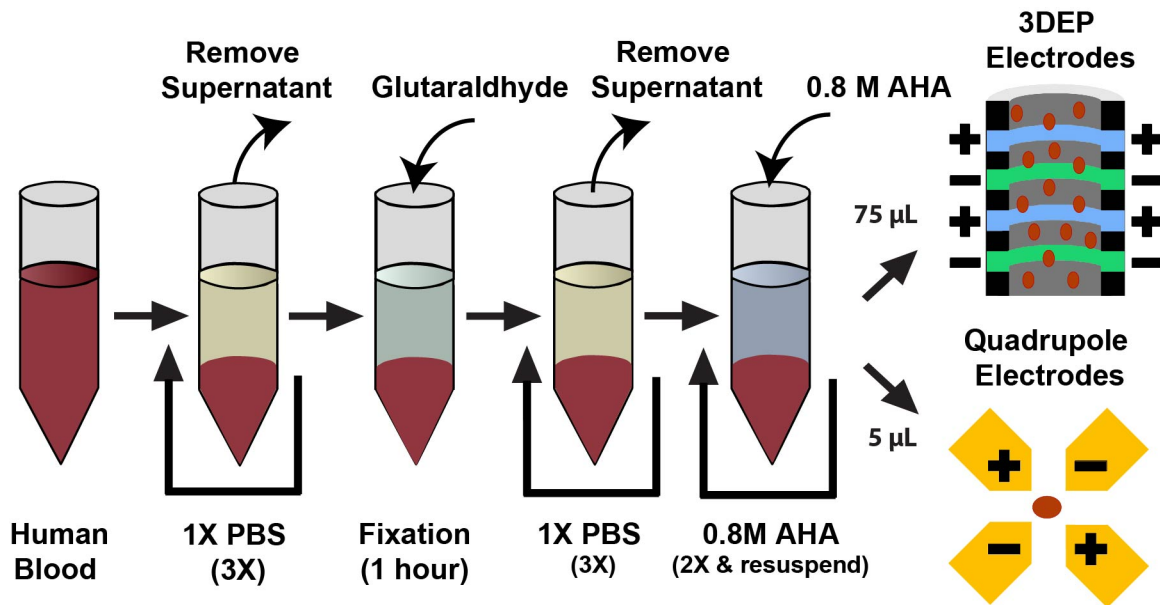
291 **3.5 High Permittivity DEP Buffer**

292 The DEP buffer used in this work was a 0.8 M 6-aminohexanoic acid (AHA)
293 (Millipore Sigma) dissolved in deionized water. The final buffer electrical conductivity
294 was controlled by first polishing the 0.8 M AHA solution for 10 min in 5g/mL Dowex
295 MR-3 ion exchange resin (Millipore Sigma) to remove trace salts, and to lower the
296 solution's electrical conductivity to a baseline value. The buffer solution electrical
297 conductivity was then adjusted to a final target value using 1X phosphate buffered
298 saline (PBS). The final DEP buffer possessed an electrical conductivity of 100 $\mu\text{S}/\text{cm}$
299 and a dielectric constant of 110, as verified in our previous electrokinetics work using
300 fluidic dielectrophoresis (fDEP) [22,23].

301 **3.6 Human Red Blood Cells**

302 Single donor O- human blood (ZenBio, Inc) was drawn intravenously in 10 mL
303 volumes and stored in DB vacutainer K2EDTA which contains di-potassium K2EDTA
304 which blocks the coagulation cascade. All human donors passed required FDA
305 screening and provided informed consent prior to blood collection. Collected blood
306 was stored in a blood bank refrigerator (Jewett) at a temperature of 4°C. Upon arrival,
307 and prior to each use, blood hematocrit was measured using pochH-100i hematology

308 analyzer (Sysmex). A depiction of the RBC washing and crosslinking DEP workflow is
 309 shown in Fig. 2. For each DEP experiment, a 20 μ L volume of blood was removed from
 310 the vacutainer and suspended in 1X PBS. The cell suspension was then gently mixed
 311 by inverting the micro-centrifuge tube 15 times and rotating it gently for 30 seconds.
 312 The diluted whole blood suspension was then centrifuged at 2000 rcf for two minutes
 313 to pellet the RBCs and remove blood components. Then supernatant was discarded
 314 and replaced with 1X PBS and the sample was further washed for a total of three
 315 times. Cells were then either crosslinked in a dilute glutaraldehyde solution or used in
 316 DEP experiments. Prior any DEP experiment, cells were washed twice in the 0.8M
 317 AHA DEP buffer and centrifuged at 6000 rcf for two minutes to remove trace amounts
 318 of 1X PBS prior to dielectrophoretic characterization. The final washed RBCs were
 319 then immediately used in the DEP experiments.



320

321

322 **Figure 2. Human RBC glutaraldehyde crosslinking workflow. Whole human**
 323 **blood is washed three times in 1X PBS and subjected to chemical fixation for 1**
 324 **hour. The cells are washed three times again in 1X PBS, washed twice in DEP**
 325 **buffer, and suspended in fresh DEP buffer for immediate DEP analysis.**

326

327 **3.7 Glutaraldehyde Crosslinking**

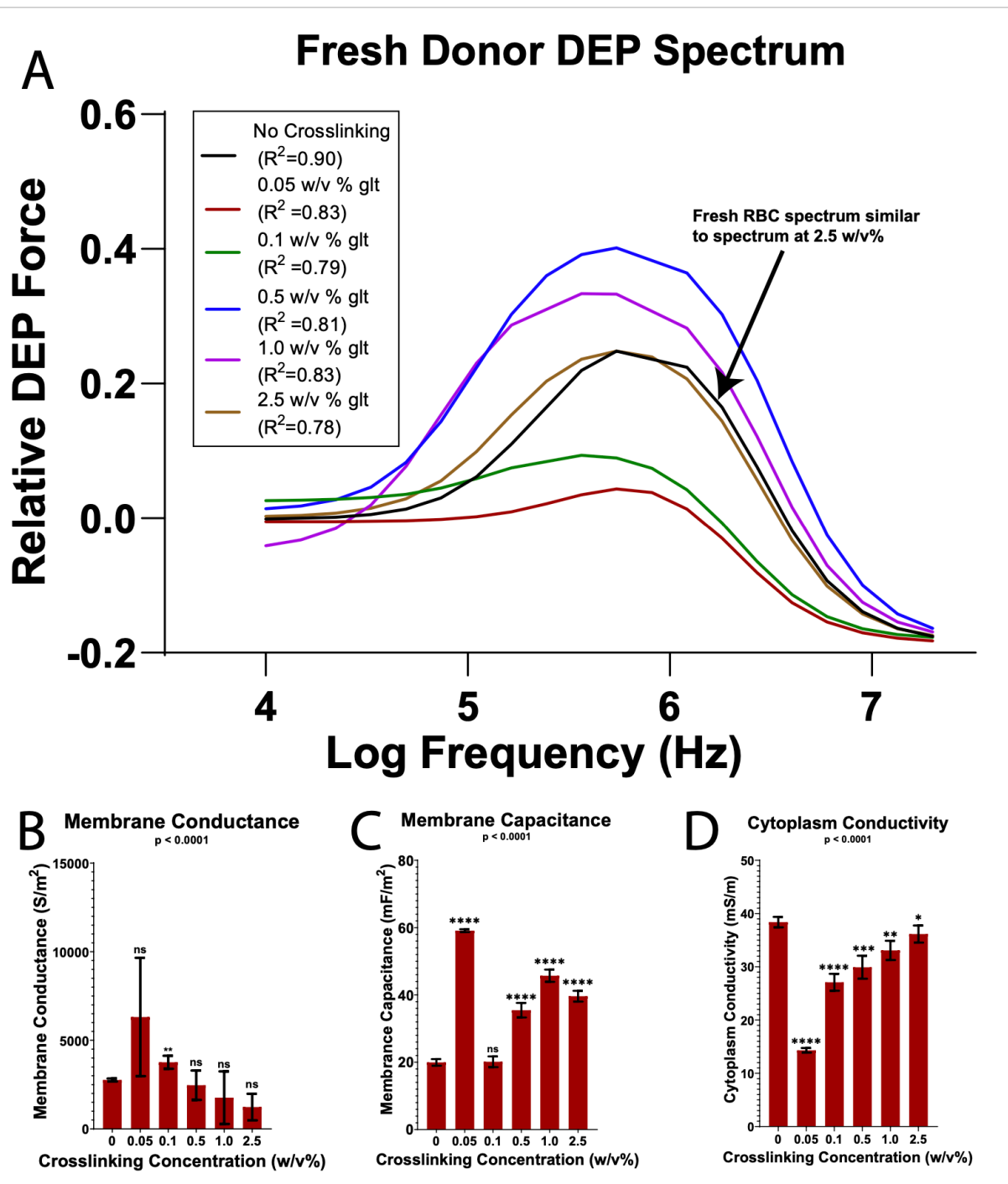
328 Following the RBC wash in 1X PBS, cells were chemically crosslinked in
329 glutaraldehyde in a similar manner as described previously [15,21]. As shown in the
330 experimental workflow in Fig. 2, glutaraldehyde (EM Grade, 25%; Polysciences, Inc)
331 was performed by first adjusting RBC concentration to 10^6 cells/ml in a 1X PBS
332 solution. A 25 w/v% glutaraldehyde stock solution was used to produce varying RBC
333 crosslinking concentrations (0, 0.05, 0.1, 0.5, 1.0, and 2.5 w/v %). Crosslinking
334 reactions were performed atop a shaker (Standard Analog Shaker 3500, VWR) for 1
335 hour at 250 rpm. To quench the crosslinking reaction, samples were centrifuged at
336 2000 rcf for 2 minutes and the supernatant was replaced with 1X PBS. After three 1X
337 PBS wash cycles, the samples were washed twice with 0.8M AHA DEP buffer and
338 then suspended in fresh 0.8M AHA DEP buffer for immediate DEP analysis.

339

340 **3.8 DEP Experiments**

341 Blood aliquots were collected after fixed storage time points (1, 5, 10, 15 and 20
342 days) after the blood draw and crosslinked. DEP analysis with the 3DEP and 2D
343 electrodes were performed immediately after PBS and AHA washing. For 3DEP
344 experiments, a gel loading pipette tip was used to load 75 μ L of a RBC suspension
345 into a 3DEP 806 chip (DEPtech, Heathfield, UK). The top surface of the chip was then
346 covered with a 20x20 mm glass coverslip and loaded into the 3DEP reader. The pin
347 connections between the 3DEP reader and the DEP chip then delivered an AC
348 potential to each of the 20 chip pinholes for 30 seconds. This experiment resulted in a
349 point-wise dataset for a relative DEP force spectrum (Fig. 1C). To improve accuracy
350 the experiment was repeated, for example $N = 7$ times, and the combined dataset was
351 regressively fit to the single-shell polarization model and used to deduce the RBC

352 electrical properties (Fig. 1D). This process was then repeated across varying RBC
 353 storage time and glutaraldehyde crosslinking concentrations.



354

355 **Figure 3. DEP Spectrum and electrical properties of fresh donor RBCs. (A)** 3DEP
 356 model spectra of RBCs for varying glutaraldehyde concentrations, $n=5$ for
 357 crosslinked, and $n=10$ for no crosslinked RBCs (B) RBC membrane
 358 conductance, (C) RBC membrane capacitance, and (D) RBC cytoplasm
 359 conductivity (b-d represent mean \pm SEM, $n=5$ for cross-linked, $n=10$ for no
 360 crosslinking, and $p < 0.0001$ by one-way ANOVA and compared to w/v% control

361 using an unpaired t test with Welch's correction (****, ***,**, and * and
362 correspond to p values < 0.0001, 0.001, 0.01, 0.05 and ns denotes p > 0.5).
363

364 4 Results and discussion

365 4.1 3DEP Spectra of Fresh Donor Cells

366 The 3DEP spectra of fresh single donor human RBCs was first measured at
367 different glutaraldehyde crosslinking concentrations. Shown in Fig. 3A., the DEP
368 spectrum of fresh donor cells is plotted for varying glutaraldehyde concentrations. For
369 fresh RBCs, the DEP spectrum of non-crosslinked cells closely mimics the spectrum
370 measured for fresh cells crosslinked at 2.5 w/v%, as indicated by the two overlapping
371 spectra. Each fresh RBC spectrum then was used to calculate the cell membrane
372 conductance (Fig. 3B), membrane capacitance (Fig. 3C), and cytoplasm conductivity
373 (Fig. 3D). For each 3DEP spectrum fitting experiment, the mean value of the cell radius
374 was measured using the sample population. Shown in Fig. 3B, the cell membrane
375 conductance initially increased and then decreased with continued increases in
376 glutaraldehyde concentrations, and finally plateaued above a glutaraldehyde
377 concentration greater than 0.5 w/v%. We observe an inverse trend with membrane
378 capacitance above concentrations of 0.05 w/v%, as capacitance steadily increased
379 with glutaraldehyde concentration from 19 mF/m² to 41 mF/m² between 0.1 w/v% and
380 2.5 w/v% and was observed to stabilize at concentrations above 0.5 w/v% (Fig. 3C).
381 Finally, we observed an initial drop in cytoplasm conductivity at a low 0.05 w/v%
382 crosslinking concentration followed by a steady increase with increasing crosslinking
383 concentrations (Fig. 3D). As observed from the measured spectra, the use of the high
384 permittivity DEP buffer enabled both the low and high frequency COFs and a
385 significant portion of the high frequency DEP spectrum to be measured within the 45
386 MHz bandwidth of the 3DEP. These experiments demonstrate that a glutaraldehyde

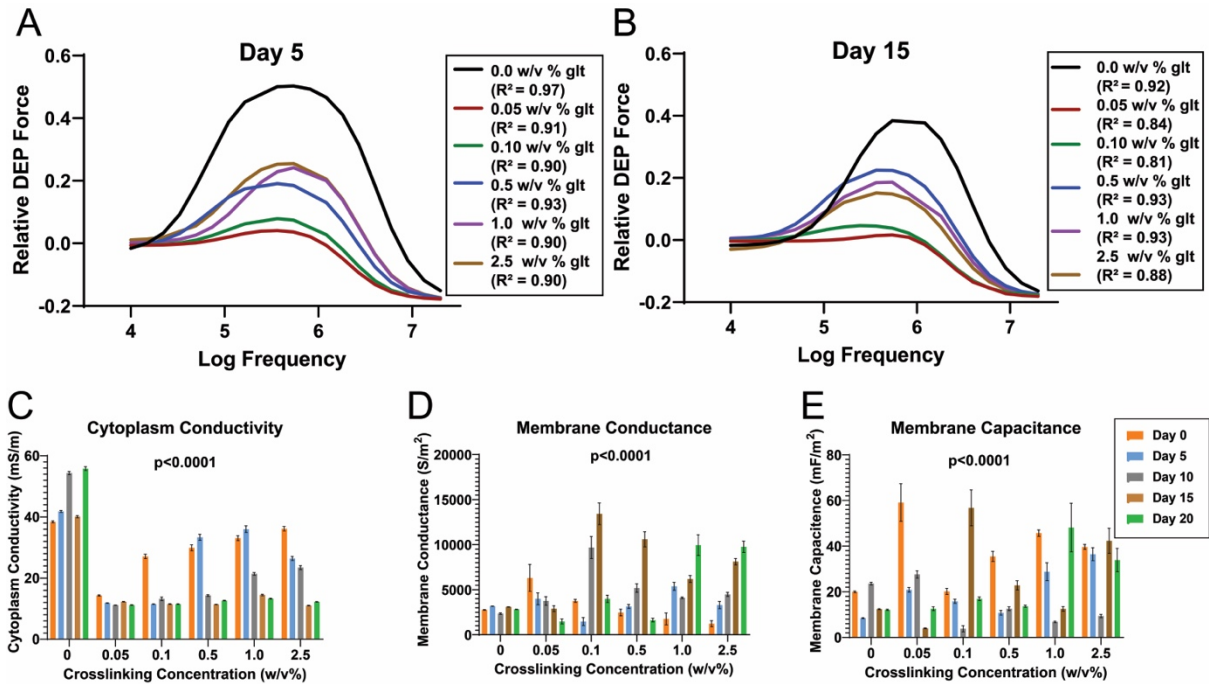
387 crosslinking concentration of 2.5 w/v% is likely to fully crosslink the RBC, as indicated
388 by the observation that cell membrane electrical properties stabilize and plateau with
389 crosslinking concentrations between 1.0 and 2.5 w/v%. These results also suggest
390 these higher concentrations serves to prevent membrane ion leakage during DEP
391 analysis as indicated by the cytoplasm conductivity at 2.5 w/v% approaching to within
392 5% of the original non-crosslinked RBC values. It is therefore anticipated that a
393 crosslinking concentration of 2.5 w/v% provides the most optimum crosslinking
394 concentration for our DEP analysis.

395

396 **4.2 DEP Analysis of Stored RBCs**

397 RBCs were stored and subsequently washed and crosslinked according to the
398 workflow presented in Fig. 2. The DEP spectrum was measured after 5, 10, 15 and 20
399 days of refrigeration. Select spectra obtained for storage times of 5 and 15 days across
400 five glutaraldehyde concentrations are plotted in Fig. 4A and 4B, respectively, to
401 illustrate the 3DEP data collection workflow. As shown, the spectra are dependent on
402 both the storage time and the glutaraldehyde concentration. In order to validate the
403 3DEP method with that of the DEP quadrupole method that was used in our previous
404 bovine RBC work, we measured the high frequency COF for both fresh and stored
405 RBCs at storage time points of 5, 10 and 15 days for all crosslinking concentrations.
406 DEP motion within the quadrupole was observed under brightfield microscopy. The
407 AC field frequency for when the first RBC “crossed over” from the quadrupole high
408 field region to the low field region, and later the frequency where the last cell crossed
409 over, was optically determined and measured. The average of these two values was
410 plotted as the high frequency COF and compared with the COF measured by the
411 3DEP. As shown in Fig. 5 for fresh RBCs (day 0), and cells stored for 5 and 15 days,

412 the 3DEP COFs agree well with the values obtained by the 2D quadrupole across all
 413 measured glutaraldehyde concentrations. As such, we believe the 3DEP instrument is
 414 a more complete DEP measurement method when compared to point-wise COF
 415 measurements obtained with 2D electrode arrays.



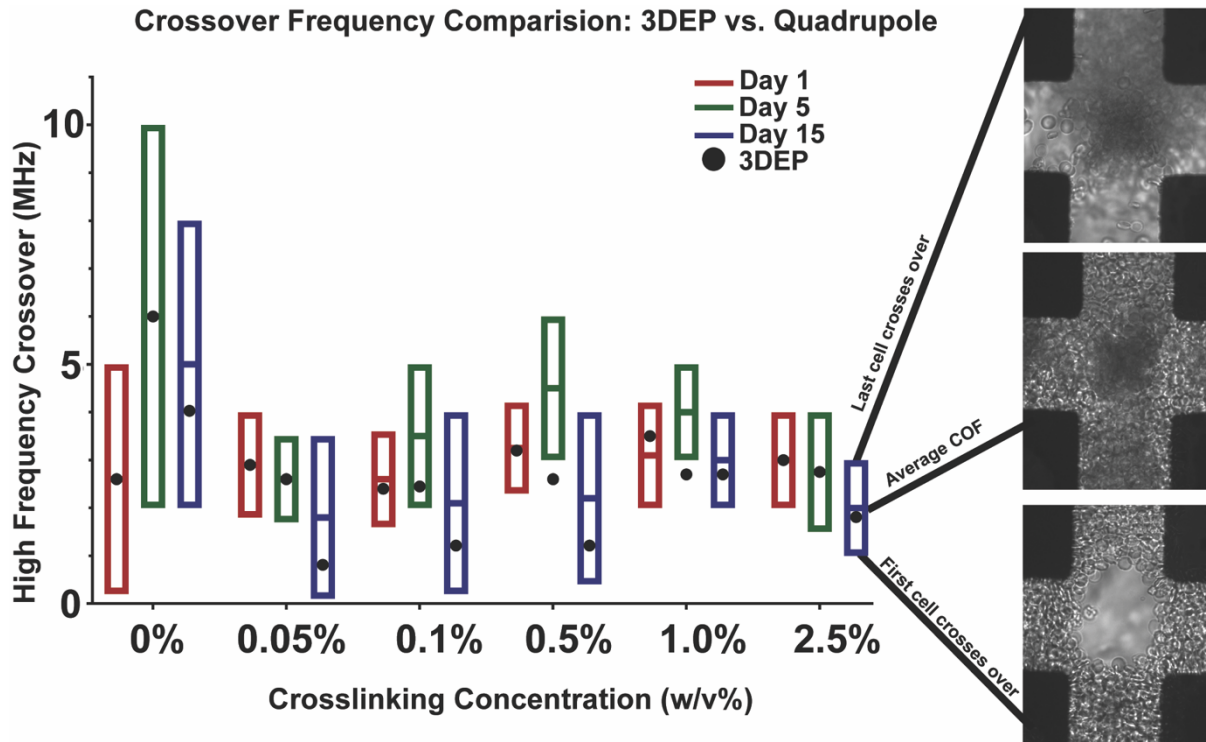
416

417 **Figure 4. 3DEP spectra and electrical properties of stored human RBCs. (A)**
 418 **3DEP spectrum for RBCs stored 5 days. (B) 3DEP spectrum for RBCs stored 15**
 419 **days. (C) RBC cytoplasm conductivity, (D) RBC membrane conductance and (E)**
 420 **RBC membrane capacitance showed statistical significance from a ordinary**
 421 **two-way ANOVA analysis with $p < 0.0001$ for both the row and column**
 422 **interactions; average +/- SEM, and $n=10$ for 0 w/v% otherwise $n=5$.**

423

424 The 3DEP was then utilized to deduce the RBC cytoplasm conductivity,
 425 membrane conductance and membrane capacitance across the varying
 426 glutaraldehyde concentrations and storage times. As shown in Fig. 4C-D, and as
 427 observed in previous work with bovine RBCs, no discernable different in RBC electrical
 428 properties was observed with human RBC storage age at a 0 w/v% glutaraldehyde
 429 concentration. However, the discernment between storage-induced RBC cytoplasm
 430 conductivity and membrane conductance increased with glutaraldehyde concentration

431 (Fig. 4C-D). As observed, the optimum crosslinking concentration for human RBC
 432 DEP resolution occurs at a glutaraldehyde concentration between 1.0 and 2.5 w/v%
 433 and is very similar to what was observed in previous crosslinking DEP experiments
 434 with bovine RBCs [15,21].



435

436 **Figure 5. Human RBC Crossover comparison between 3DEP spectrums and 2D**
 437 **quadrupole array for RBCs at day 1, 5 and 15 of storage.**

438

439

440

441

442

443

444

445

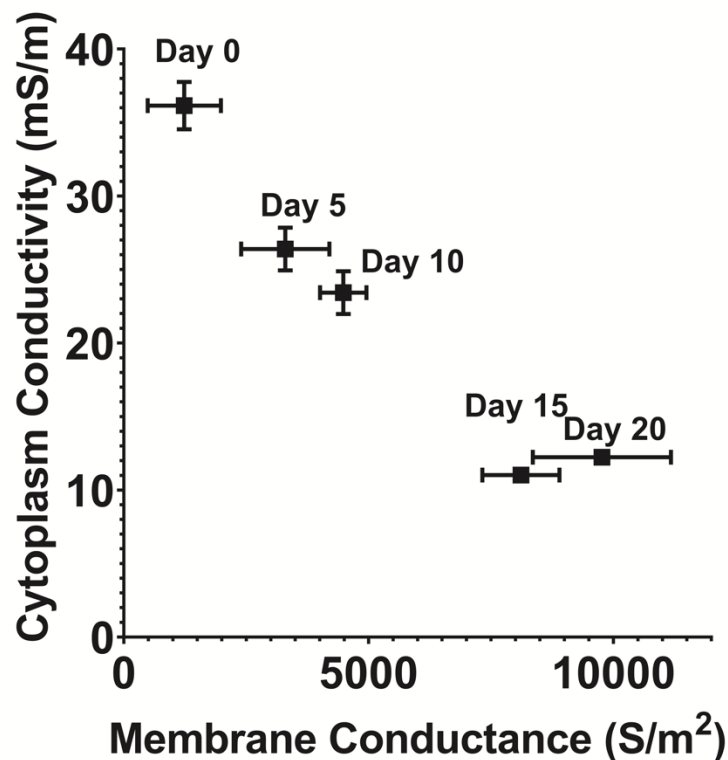
446

447

The RBC cytoplasm conductivity and membrane conductance exhibited observable trends with increasing storage time at a glutaraldehyde concentration of 2.5 w/v% (Fig. 4C-E). Here, the cytoplasm conductivity was observed to steadily decrease from an initial value of 0.036 S/m to 0.026, 0.023, 0.011, and 0.012 S/m with increasing storage times of 5, 10, 15 and 20 days, respectively. Conversely, the membrane conductance was observed to increase with increasing storage time, increasing from an initial value of 500 S/m² to 3000, 5000, 10,000, 12,000 S/m², at storage times of 5, 10, 15, and 20 days, respectively. Interestingly, the membrane

448 conductance appears to have an inverse relationship with the cytoplasm conductivity,
449 as shown in Fig 6. While this trend presented is from a single human donor, this
450 inverse relationship between cytoplasm conductivity and membrane conductance was
451 been consistently observed with 9 total blood donors that were studied using this DEP
452 method. However, a more detailed investigation into the DEP variability in electrical
453 properties and COF across the human donors will be the subject of a future study. The
454 inverse correlation between decreasing conductivity and increasing conductance has
455 also been observed in other DEP work. In Henslee et al. for example, the authors
456 showed an anti-phase relationship between these two electrical parameters [5]. We
457 speculate here that this inverse trend is driven by the single-shelled relationship
458 between the cell cytoplasm conductivity and the surrounding cell membrane. In the
459 absence of cell hemolysis, a main driver for ion transport and a decrease in RBC
460 cytoplasm conductivity during refrigerated storage is diffusive ion flux from the
461 cytoplasm and across the cell membrane through the physical migration of ions across
462 this domain. Ionic concentration within the cell membrane would therefore increase
463 during this process and subsequently lead to an increase in membrane conductance.
464 Further storage experiments using both dynamic DEP measurements and inductively
465 coupled plasma mass spectrometry (ICP-MS) are needed to better understand the
466 relationship between RBC DEP and ionic composition overtime and will be the subject
467 of a future study. While a clear trend was observed between cytoplasm conductivity
468 and membrane conductance with increasing storage time, no storage time
469 dependence was observed with membrane capacitance for any experimental
470 glutaraldehyde crosslinking concentration. It is worth noting that our 3DEP measured
471 cytoplasm conductivity values ($\sim 10 - 40$ mS/cm) are lower than values reported
472 elsewhere (~ 100 mS) for human RBCs [5]. While our results demonstrate that

473 glutaraldehyde is capable of minimizing dynamic ion leakage across RBCs, the cell
474 handling conditions may also contribute to the electrical state of the RBCs. These
475 conditions were held constant when RBCs were washed and crosslinked for this work,
476 however, an understanding of how varying centrifuge conditions and incubation
477 temperatures ultimately influence RBC electrical properties is likely warranted to better
478 understand this observed electrical. Previous reported values, for example, were
479 acquired after RBCs had been incubated at 35 – 37 °C for 48 h [5], while this DEP
480 work maintained cell samples at a continuous refrigerated temperature of 4 °C. We
481 therefore believe that cell handling and incubation conditions can strongly influence
482 the RBCs electrical state and can give rise to measured differences such as what is
483 observed here.



484

485 **Figure 6. RBC cytoplasm conductivity decreases with increasing membrane**
486 **conductance with increasing storage time.**

487

488 The 3DEP was able to resolve the electrical property changes in single-donor
489 human RBCs with increasing storage time using a chemical crosslinking method. The
490 cell crosslinking reaction served to prevent ionic leakage across the cell membrane
491 during DEP analysis and therefore the cellular ionic composition more accurately
492 represented that which existed in the original storage buffer prior to crosslinking. It is
493 well known that RBC ion channels are sensitive to changes in temperature and human
494 red blood cells leak potassium ions during storage [12]. Ion leakage such as this would
495 likely lead to a reduction in the cytoplasm conductivity and an increase in ionic species
496 within the cell membrane. If, however, glutaraldehyde was not utilized in this work, the
497 ion depleted cytoplasm and ion accumulated membrane would dynamically respond
498 to a resuspension in the low conductivity DEP buffer and dynamically reach a new
499 ionic equilibrium with their surroundings. Such communication with the surrounding
500 cell buffer would ultimately lead to an internal cytoplasm conductivity that is not
501 representative of the leakage that occurred during the storage process.

502 Glutaraldehyde is a well understood cell fixation agent which crosslinks the
503 aminated protein groups of the RBC [24]. These results suggest that the
504 polymerization of the cell membrane significantly reduces the rate of ion leakage
505 across the cell membrane during DEP analysis if a large enough crosslinking
506 concentration is utilized. In this work, DEP resolution occurred at crosslinking
507 concentrations above 1.0 w/v%. Below this concentration a trend emerged
508 dynamically and became discernable in a manner that was dependent of the age of
509 the RBC sample. In particular, the initial observable trend for the cytoplasm
510 conductivity was strongly influenced by RBC storage time. No age-related trend was
511 observable in RBCs without crosslinking, but a measurable difference in cytoplasm
512 conductivity was first observed with the youngest RBC populations. Shown in Fig. 4C,

513 a crosslinking concentration of 0 and 0.05 w/v% showed no observable change in
514 conductivity with storage time. However, at a concentration of 0.1 w/v% a difference
515 in cytoplasm conductivity was observable for a single sample: fresh day 1 cells.
516 Interestingly, the sample storage age in which a measurable difference was first
517 observed increased with increasing crosslinking concentration. At a concentration of
518 0.5 w/v%, for example, day 0 and day 5 RBCs exhibited measurable differences in
519 cytoplasm conductivity, while the remaining cell sample storage times showed no
520 discernable electrical differences at this crosslinking concentration. Further increases
521 in crosslinking concentration (>1.0 w/v%) then produced observable differences in the
522 cytoplasm conductivity across the entire experimental time course. Given that the
523 RBCs shed membrane proteins during storage, fewer available crosslinking sites are
524 available as storage age increases. We observe here that a smaller crosslinking
525 concentration is required to influence ionic leakage in “fresh” cells than what is
526 required for cells stored at the longer 5-, 10- and 20-day timepoints. This interplay
527 between storage age and minimum crosslinking concentration for preventing cell
528 leakage is therefore likely due to the age-dependent availability of RBC aminated
529 crosslinking sites. While clear statistically significant differences in RBC cytoplasm
530 conductivity and membrane conductance are observable over a refrigeration period of
531 20 days at crosslinking concentrations > 1.0 w/v%, no such difference was detected
532 in the membrane capacitance over this period for any concentration. As such, it is
533 likely refrigerated RBC storage over a period of 20 days did not significantly alter the
534 membrane permittivity, thickness or cell surface area to the extent to which a change
535 in membrane capacitance could be detected by the 3DEP.

536 **5 Concluding remarks**

537 In this work, we have presented a glutaraldehyde chemical crosslinking method
538 for the detection of human RBC electrical properties by DEP. Single donor type O-
539 human RBCs were stored in a blood bank refrigerator over a period of 20 days. Blood
540 samples were withdrawn from refrigerated storage at varying time points 0, 5, 10, 15,
541 and 20 days and chemically crosslinked in varying concentrations of glutaraldehyde
542 ranging from 0 w/v% - 2.5 w/v%. Crosslinked cells were then suspended in a high
543 permittivity 0.8M AHA buffer in order to increase the buffer permittivity and
544 subsequently reduce the frequency bandwidth required to obtain a full DEP spectrum.
545 Using this chemical crosslinking high permittivity buffer system, we performed human
546 RBC DEP analysis using a commercial 3DEP instrument. The high frequency COF
547 obtained using the 3DEP method was compared and shown to agree well with the
548 COF values obtained using a conventional 2D quadrupolar electrode array. DEP
549 spectra from 3DEP experiments were measured and fitted using nonlinear regression
550 to a spherical single-shell polarization model in order to determine the RBC cytoplasm
551 conductivity, membrane conductance and membrane capacitance over a period of 20
552 days of refrigerated storage. We show that at chemical crosslinking concentrations
553 above 1.0 w/v%, 3DEP analysis yielded discernable differences in cell electrical
554 properties with increasing storage time. In particular, the RBC cytoplasm conductivity
555 was observed to increase while the membrane conductance decreased with
556 refrigerated storage time. No trend was observed in RBC membrane capacitance with
557 increasing storage time. Further, no RBC electrical differences were resolvable by
558 DEP without glutaraldehyde crosslinking. The chemical crosslinking approach serves
559 to eliminate ionic diffusion across the cell membrane when cells are resuspended in
560 DEP buffer for analysis. Therefore, this chemical crosslinking method enables the

561 discernment of electrical property changes during storage and prevents cells from
562 reestablishing ionic equilibrium with the low conductivity DEP buffer. This assay can
563 successfully detect differences in blood storage, or starvation age, which is currently
564 challenging to perform using patch clamp or single cell electrophysiology techniques.
565 Interestingly, an inverse relationship between cytoplasm conductivity and membrane
566 conductance is observed. This work offers a robust method for characterizing the
567 quality of blood electrically and has applications in blood transfusion storage logistics
568 and for detecting age related electrical property changes in blood samples from
569 endurance athletes which have undergone illegal autologous blood transfusions.
570 Future efforts will focus on better understanding the species involved with ionic
571 leakage and understanding how these measurements vary across human donors.

572 **Acknowledgements**

573 The authors acknowledge funding and support from the Partnership for Clean
574 Competition (PCC) and the World Anti-Doping Agency (WADA).

575 **Conflict of interest**

576 The authors declare no financial interest.

577 **Data Availability Statement**

578 The data that support the findings of this study are available from the corresponding
579 author upon reasonable request.

580 **6 References**

581 [1] Labeed, F. H., Lu, J., Mulhall, H. J., Marchenko, S. A., Hoettges, K. F., Estrada,
582 L. C., Lee, A. P., Hughes, M. P., Flanagan, L. A. *PLoS ONE* 2011, 6, e25458.

- 583 [2] Jiang, A. Y. L., Yale, A. R., Aghaamoo, M., Lee, D. H., Lee, A. P., Adams, T. N.
584 G., Flanagan, L. A. *Biomicrofluidics* 2019, 13.
- 585 [3] Gascoyne, P., Satayavivad, J., Ruchirawat, M., *Acta Tropica* 2004, 89, 357-369
- 586 [4] Mahabadi, S., Labeed, F. H., Hughes, M. P. *Electrophoresis* 2018, 39, 1104–
587 1110.
- 588 [5] Henslee, E. A., Crosby, P., Kitcatt, S. J., Parry, J. S. W., Bernardini, A., Abdallat,
589 R. G., Braun, G., Fatoyinbo, H. O., Harrison, E. J., Edgar, R. S., Hoettges, K. F.,
590 Reddy, A. B., Jabr, R. I., Schantz, M. von, O'Neill, J. S., Labeed, F. H. *Nature*
591 *Communications* 2017, 8.
- 592 [6] Huang, C., Chen, A., Wang, L., Guo, M., Yu, J. *Biomedical Microdevices* 2007,
593 9, 335–343.
- 594 [7] Huang, C., Chen, A., Wang, L., Guo, M., Yu, J. *Biotechnology letters* 2007, 29,
595 1307–1313.
- 596 [8] Mahabadi, S., Labeed, F. H., Hughes, M. P. *Electrophoresis* 2018, 39, 1104–
597 1110.
- 598 [9] Flanagan, L. A., Lu, J., Wang, L., Marchenko, S. A., Jeon, N. L., Lee, A. P., &
599 Monuki, E. S. *Stem cells* 2008, 26, 656–665
- 600 [10] Zimrin, A. B., Hess, J. R. *Vox Sanguinis* 2009, 96, 93–103.
- 601 [11] Hess, J.R. *Vox Sanguinis* 2014, 107, 1–9.
- 602 [12] Kfoury Baz, E. M., Kanazi, G. E., Mahfouz, R. A. R., Obeid, M. Y. *Transfusion*
603 *Medicine* 2002, 12, 383–386.
- 604 [13] Pohl, H. A. *Journal of Applied Physics* 1951, 22, 869–871.
- 605 [14] Hoettges et al, *Sci Rep* 2019, 9, 19153.
- 606 [15] Gordon, J. E., Gagnon, Z., Chang, H. C. *Biomicrofluidics* 2007, 1, 044102.
- 607 [16] Gagnon, Z., Gordon, J., Sengupta, S., Electrophoresis, H. C.-, 2008, undefined
608 *Wiley Online Library* 2008, 29, 2272–2279.
- 609 [17] Gagnon, Z., Mazur, J., Chang, H. C. *Biomicrofluidics* 2009, 3, 044108.
- 610 [18] Gagnon, Z. R. *Electrophoresis* 2011, 32, 2466–2487.
- 611 [19] Pethig, R. *Biomicrofluidics* 2010, 4, 022811.
- 612 [20] Cottet, J., Fabregue, O., Berger, C., Buret, F., Renaud, P., Frénéa-Robin, M.
613 *Biophysical Journal* 2019, 116, 12–18.

- 614 [21] Gagnon, Z., Gordon, J., Sengupta, S., Chang, H.-C. *Electrophoresis* 2008, 29,
615 2272–2279.
- 616 [22] Mavrogiannis, N., Desmond, M., Gagnon, Z. R. *Electrophoresis* 2015, 36, 1386–
617 1395.
- 618 [23] Desmond, M., Mavrogiannis, N., Gagnon, Z. *Physical Review Letters* 2012, 109.
- 619 [24] Cheung, D., Nimni, M., *Connective tissue research* 1982, 10, 187–199.
- 620